
This is the **accepted version** of the journal article:

Rodrigues, Ana Luísa; Marques, Rosa; Dias, Maria Isabel; [et al.]. «Luminescence and compositional studies for the identification of "fire-setting" features at prehistoric mine La Turquesa (Catalonia, Spain)». *Journal of Radioanalytical and Nuclear Chemistry*, Vol. 331 Núm. 3 (2022), p. 331-1408. 12 pàg. DOI 10.1007/s10967-022-08198-0

This version is available at <https://ddd.uab.cat/record/289404>

under the terms of the  license

1 **Luminescence and compositional studies for the**
2 **identification of “fire-setting” features at prehistoric**
3 **mine La Turquesa (Catalonia, Spain)**

4 Ana Luísa Rodrigues^{1*}, Rosa Marques^{1,2}, Maria Isabel Dias^{1,2}, Maria Isabel Prudêncio^{1,2},
5 Guilherme Cardoso³, Dulce Russo^{1,2}, Núria Rafel Fontanals⁴, Eni Soriano⁵

6

7 ¹*Centro de Ciências e Tecnologias Nucleares (C2TN), Instituto Superior Técnico,*
8 *Universidade de Lisboa, E.N. 10 (km 139,7), 2695-066 Bobadela, Portugal*

9 ²*Departamento de Engenharia e Ciências Nucleares (DECN), Instituto Superior Técnico,*
10 *Universidade de Lisboa, E.N. 10 (km 139,7), 2695-066 Bobadela, Portugal*

11 ³*Divisão de Planeamento e Proteção Radiológica, Departamento de Emergência e*
12 *Proteção Radiológica, Agência Portuguesa do Ambiente*

13 ⁴*Universitat de Lleida, Facultat de Geografia i Història, plaça Víctor Siurana 1, 25003*
14 *Lleida, Spain*

15 ⁵*Departament de Prehistòria, Universitat Autònoma de Barcelona, Edifici B, 08197*
16 *Bellaterra, Spain*

17 *corresponding author: Ana Luísa Rodrigues, alsr@ctn.tecnico.ulisboa.pt, (+351) 219
18 946 224

19

20

21 **Abstract**

22 Modern mining activities often leads to destruction of archaeological records, making
23 difficult to date the contexts and tools. In this work, a prehistoric mine with “fire-setting”
24 techniques evidence was used to demonstrate the relevance of luminescence protocols to
25 identify and date ancient mining activities. Chemical and mineralogical studies
26 complemented the dosimetric ones by means of luminescence protocols. One of the
27 samples shows lower absorbed dose suggesting heating procedures, like “fire-setting” and
28 its luminescence age, determined by SAROSL, points to copper exploitation during the
29 Middle/Late Bronze Age at La Turquesa mine, in accordance with archaeological records.

30 **Keywords**

31 Prehistoric mining, “Fire-setting”, Luminescence protocols, Luminescence dating,
32 Geochemistry

33 **Introduction**

34 “Fire-setting” is well recognized as one of the oldest mining techniques for breaking up
35 hard rocks and extract the ore, mostly in open mines of northern Europe, and was identified
36 since prehistoric times up to the 19th century [1, 2]. Fires were set against a rock face to
37 heat it; it was then doused with liquid, usually water, causing the rock to weaken and
38 fracture due to the thermal shock. The technique is usually associated with mechanical
39 methods (hammering, picking, wedging, etc.). The use of “fire-setting” in European
40 prehistoric copper mines was clearly identified in mining districts of France (Cabrières and
41 Faravel), Austria (Mitterberg and Tyrol), Ireland (Mt. Gabriel mines), Wales, former
42 Yugoslavia (Rudna Glava) and Spain (Aramo mine in Asturias) [2–7]. The main evidence
43 of the use of “fire-setting” in ore exploitation is the presence of meter-sized spherical or
44 sub-spherical cavities, sometimes spaced along the same vertical line in an ore seam,
45 together with charcoal and traces of fire. The wood fire, generally associated to this

46 technique, lead to a range of temperatures between 100 °C to 600 °C with different effects
47 in the parent material [2].

48 The few existing studies regarding exploitation techniques in prehistoric mines are mainly
49 focused on mineralogical and chemical alterations of the rock, the used fuel, the achieved
50 temperatures, the gradient temperature inside the rock, the procedures, the study of tools
51 and charcoal finds, as well as experimental simulation [2, 5, 8, 9]. A different approach
52 was applied to the prehistoric mines of the French and Austrian Alps, including
53 anthracological and dendrochronological analysis of wood remains, in order to evaluate
54 the chronology of the exploitation and the impact of the mining economy in the region [5–
55 7, 10].

56 There is a lack of chronological data for this type of archaeological context, particularly
57 related with the moment of the technological event, relevant to ancient mining and
58 metallurgy activities. When organic materials are available in mining contexts, such as
59 wooden tools, mining tools, or firewood and charcoal, ¹⁴C dating is usually used [5, 11,
60 12]. However, these materials are rare in mines and their contexts were disturbed by the
61 alternated periods of exploitation vs abandonment. In addition, a complex stratigraphy and
62 diverse reuses over time are associated with these mining contexts, making the absolute
63 dating difficult[13]. Nevertheless, working techniques remains and associated inorganic
64 materials can be studied by using luminescence techniques [14]. A few dating attempts of
65 the last heating of feldspars and quartz (e.g. in slags or in rocks) have been done in mining
66 contexts with “fire-setting” evidence [4]. Studies applying luminescence protocols on
67 quartz, polymineralic and alkali feldspars fractions from burnt rocks, heated flint and fire-
68 cracked rocks of prehistoric human occupations are well described [15–19]. Luminescence
69 was also used to assess the reached temperature on fired rock surfaces and dating fires on
70 historical buildings [20].

71 Recent archaeological work in La Turquesa mine (also known with the name of Mas de les
72 Moreres mine), Cornudella de Montsant, Catalonia, Spain (coordinates: ETRS89:
73 UTM31N, 323884.605/4566667.437), where secondary copper ores were exploited,
74 reveals sub-elliptical or sub-spherical cavities on the rock, pointing to the use of “fire-
75 setting” techniques during pre-industrial mining activities [21]. La Turquesa mine is
76 located on the south-western sector of the Pre-Litoral Range, containing the southernmost

77 outcrops of Palaeozoic rocks in the Catalan Coastal Ranges. Based on a previous work
78 developed on rock samples from a similar archaeological site [14], the authors performed
79 a preliminary study, in which a thermoluminescence protocol was applied [22]. This first
80 approach points to the use of heating processes against the rock surface.

81 In this work, an innovative and detailed study is performed, with the main goal of testing
82 luminescence techniques as a reliable tool to confirm the practice of “fire-setting”, and
83 aiming to better establish the use of “fire-setting” techniques in ancient mining activities.

84 In order to complement the luminescence analysis, a more detailed characterization of La
85 Turquesa mine is done with the determination of the chemical composition of rock
86 fragments from two mining shafts and geological background, and the correlation with the
87 mineralogical composition of the materials.

88

89 **Geo-archaeological context**

90 La Turquesa mine has morphological features and archaeological remains usually
91 associated to the use of “fire-setting” during pre-industrial mining activities [21]. This mine
92 is located at the southwestern sector of the Pre-Litoral Range, where the southernmost
93 outcrops of Palaeozoic rocks in the Catalan Coastal Ranges are observed. Outcrops of
94 sedimentary materials from the Upper Devonian and the Carboniferous also occur. These
95 series were deformed by the Hercynian orogeny, and affected by contact metamorphism
96 produced by granite intrusions. The Mesozoic series uncomfortably overlies the above
97 materials and are covered in a discordant manner, by detrital series from the Tertiary
98 Period. The ensemble had been compartmented by faults from the Alpine Period [23]. The
99 deposit of La Turquesa mine was formed following a vein structure related to the main
100 Cornudella fault and has a NNW-SSE direction. The veins are hosted by chert
101 metasedimentary units of Tournaisian age that have millimeter-thick apatite beds
102 interbedded. The primary minerals are chalcopyrite and pyrite disseminated in milky
103 quartz. The supergene alteration produced a gossan zone with goethite, malachite, azurite
104 and cuprian crandallite. The gossan evolves at 3 m in depth, to a supergenic enrichment
105 zone with Cu-rich sulphides as chalcocite, which replaces the primary chalcopyrite. La
106 Turquesa mine was opened to exploit secondary copper ores, located in the upper part of a

107 vein zone with pyrite and primary chalcopyrite that, due to supergene alteration, results in
108 a gossan with crandallite and malachite, accompanied by minerals of the alunite group, and
109 a zone of supergenic enrichment with chalcocite. The indicated paragenesis has its remote
110 origin in the simultaneous meteorisation of pyrite and apatite in the hosting rocks, in one
111 hand, and of the chalcopyrite veinlets, on other hand [23].

112 Three excavation campaigns occurred in 2012, 2013 and 2015 in La Turquesa mine. These
113 campaigns allowed documenting more than a hundred mining stone tools, as well as, the
114 main copper mineralization, a mining shaft (L1), and the remains of two more mine shafts
115 (L2 and L3).

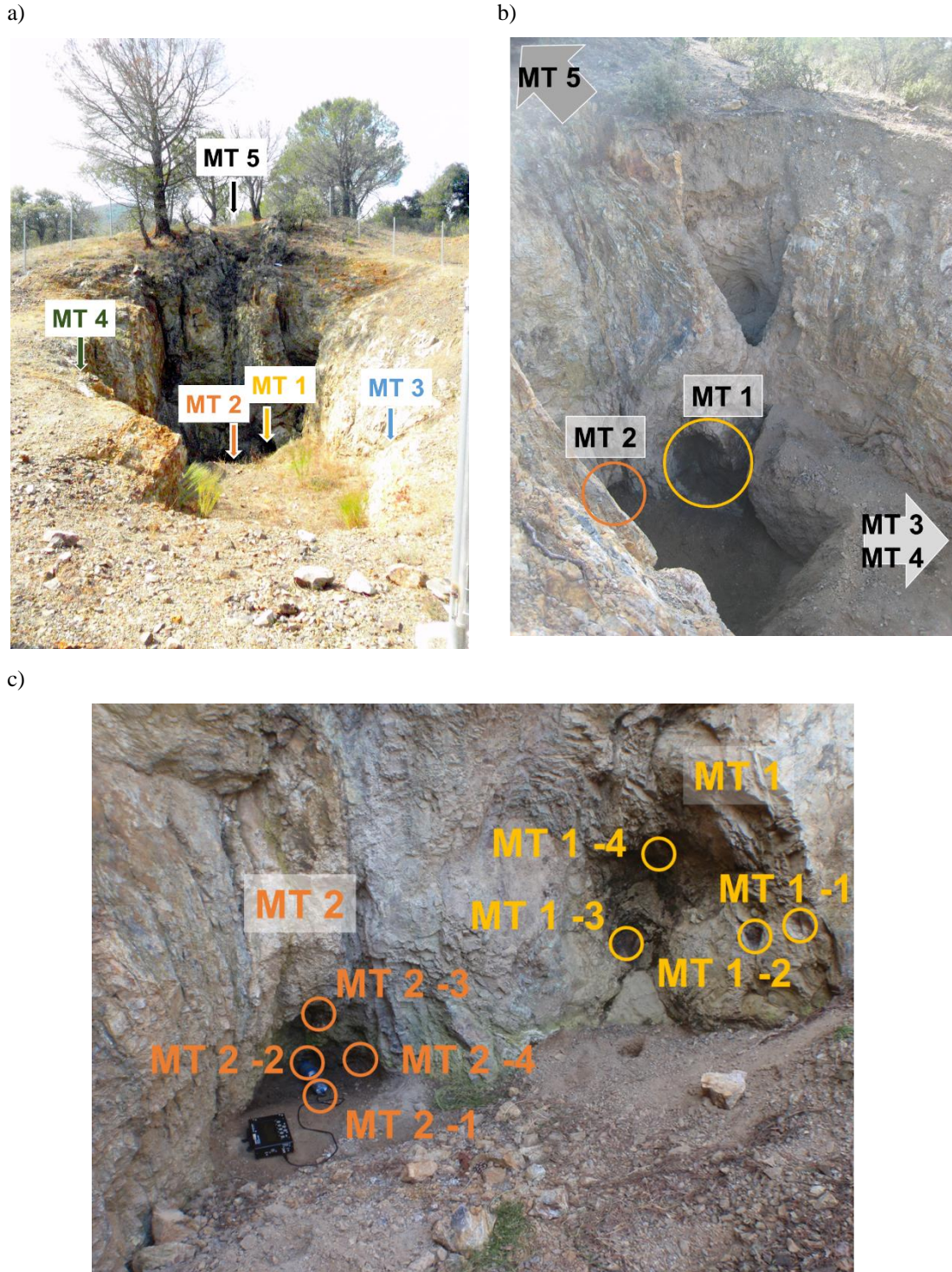
116 The chronological records established up to now for La Turquesa mine are: (i) a prehistoric
117 horizon including lithic mining prehistoric tools (picks, picks/percussors and percussors),
118 and mining working without any evidence of the use of metal-tools intervention (thus
119 excluding a post-Roman chronology); (ii) radiometric dates obtained from the infill
120 sediment of the mining shaft L1, providing a date *ante quem*, corresponding to the early
121 Middle Ages; and (iii) the consistency of isotopic signature of the mine with archaeological
122 materials, attributed to the Late Chalcolithic and to the Early-Middle Bronze Age (2800-
123 1300 cal BC) [24].

124

125 **Samples**

126 At La Turquesa mine, samples were taken from the remains of two mining shafts, L2 and
127 L3, located in the centre of the mine close to the mined Cu-vein, with evidence of pre-
128 industrial mining (Fig. 1). In addition, two representative samples from geological
129 background and one from a non-exploited section of the copper vein were collected. In
130 shaft L2, four rock fragments were sampled, corresponding to the references MT1_1,
131 MT1_2, MT1_3 and MT1_4. In shaft L3, one sediment (MT2_1) and three rock fragments
132 were collected, corresponding to the references MT2_2, MT2_3 and MT2_4 (Fig. 1). The
133 selected rock fragments are poorly indurated and break apart easily by hand, especially
134 fragment MT1_1. The sediment MT2_1 was removed using a stainless-steel tube,
135 according to the conventional sampling protocol for luminescence dating [25]. Two
136 samples from the bedrock surrounding the mine (MT3 and MT4), and one sample in the

137 copper vein (MT5) were also selected for this study (Fig. 1 and Fig.). The MT3 and MT4
138 samples were collected on the exploitation limit that corresponds to the 19th century mining
139 activities, on the western and eastern edge of the mining shaft respectively. In opposition,
140 the MT5 sample was taken on the southern edge of the Cu-vein (N-S) where no evidence
141 of mining activities was observed. The MT3, MT4 and MT5 rock fragments were collected
142 to be used as references for the luminescence signal boundaries, since it is expectable that
143 they preserve the geological signal, without consequences of heating during mining
144 processes. The MT2_1 sample, corresponding to the sediment accumulated at the shaft L3
145 after the last mining activity, is expected to have a lower luminescence signal. This sample
146 was also used as luminescence signal boundary, but with the opposite purpose, of
147 representing the material with geological signal bleached by recent sun exposure.
148



149 **Fig. 1** Photographs of samples location at La Turquesa mine, Cornudella de Montsant
150 (Catalonia, Spain): a) overview of the mine with identification of the sampling points
151 (MT1, MT2, MT3, MT4, and MT5); b) view of the mine entrance with the identification
152 of the sampling points MT1 and MT2; and c) detailed view of the shafts L2 (sampling point
153 MT1) and L3 (sampling point MT2) and the respective samples (MT1_1, MT1_2, MT1_3,
154 MT1_4; MT2_1, MT2_2, MT2_3, MT2_4).

155

a)

MT1_1

MT1_2

MT1_3

MT1_4



b)

MT2_1

MT2_2

MT2_3

MT2_4



c)

MT3

MT4

MT5



156 **Fig. 2** Details of the La Turquesa mine, Cornudella de Montsant (Catalonia, Spain)
157 samples: a) shaft L2, sampling point MT1 (samples from 1 to 4); b) shaft L3, sampling
158 point MT2 (samples from 1 to 4); and c) sampling points MT3, MT4 and MT5.

159

160 **Methodological approach**

161 The first step in the sample preparation is the removal of the outer part of the rock
162 fragments and the external part of the material collected using the stainless-steel tubes. This
163 material was used for the chemical and mineralogical analyses, being first powdered in an
164 agate mortar. The inner part of the samples was selected for luminescence analyses,
165 avoiding the analysis of grains exposed to sunlight.

166 The mineralogical composition of rock and sediment samples [22] was achieved by means
167 of X-ray diffraction (XRD), using a Philips Pro-Analytical spectrometer with a Cu-K α
168 source. Semi-quantitative analysis of mineral assemblages was undertaken by measuring
169 the principal peak areas with intensities correction, using the recommended weighting
170 factors [26–36].

171 The chemical analyses were performed at Activation Laboratories Ltd. (Actlabs) (Ontario,
172 Canada). Chemical contents of Sc, Cr, Co, As, Br, Rb, Mo, Sb, Ba, La, Ce, Nd, Sm, Eu,
173 Tb, Yb, Lu, Th and U were obtained by instrumental neutron activation analysis (INAA)
174 and the chemical content of Na₂O, MgO, Al₂O₃, SiO₂, P₂O₅, K₂O, CaO, TiO₂, V₂O₅, MnO,
175 Fe₂O_{3(Total)} and CuO by X ray fluorescence (XRF).

176 An enriched quartz coarse grains fraction of rock and sediment samples was obtained by
177 manual disaggregation using an agate mortar. From this material, the 180-250 μm fraction
178 was separated by dry sieving. A conventional laboratory procedure was applied to isolate
179 the quartz grains, by etching the samples with HCl 10 % and H₂O₂ to remove carbonates
180 and organic matter. The resulting material was washed with distilled water and a density
181 separation process with heavy liquid LST was applied to obtain the fraction between 2.61
182 gcm^{-3} and 2.70 gcm^{-3} . A final cleaning process of the quartz grains was performed by using
183 a chemical treatment with HF 40 % and HCl 10 % solutions. After washing with distilled
184 water, the enriched quartz coarse grains fraction was dried at 50 °C. To proceed to the
185 luminescence measurements, monolayers of quartz grains were fixed on stainless steel
186 discs using silicone oil (aliquots).

187 To confirm the use of “fire-setting” techniques, the evidence of heating was tested in the
188 enriched quartz coarse grains fraction by two luminescence protocols. The first one was
189 based on a previous work [14] and performed by the authors as slightly more complex
190 thermoluminescence (TL) measurements protocol for coarse quartz grains, instead of a

191 simple TL protocol applied to polymineralic samples [22]. Normally, TL measurements
192 applied to quartz enable a distinction between non-heated samples and samples heated to
193 above 300 °C, which have lower intensity in the TL signal. Thermoluminescence
194 measurements were performed according to a sequence already described in [22]. In that
195 work, for all the aliquots of each sample, the natural thermoluminescence curves (TLn)
196 were measured, and subsequently groups of four aliquots of each sample were irradiated
197 during 100, 400 and 800 s, respectively. After a pause of 12 hours, regenerative
198 thermoluminescence (TLr) curves were obtained (TLr100, TLr400 and TLr800) [22].
199 The second procedure proposed in the present work is commonly used as a semi-
200 quantitative protocol with high stratigraphic resolution in profiling studies [4, 37–40] to
201 solve chronological issues and will be applied for the first time in the identification of
202 ancient mining activities. In addition, a quantitative luminescence protocol is applied to
203 refine/confirm the chronology of the copper exploitation in this mine. Due to the
204 heterogeneous heating of the rock and the complexity of the associated protocols, this
205 approach is a challenge, with particular emphasis on the preparation of the mineral grains
206 for analysis (difficult in desegregating the rock for isolate and purify a quartz fraction). The
207 semi-quantitative luminescence protocol, using five aliquots of each sample, comprising
208 multi-signal measurements (TL, OSL and IRSL), is given in Table 1. This protocol enables
209 the evaluation of dominant luminescence signals to guide subsequent quantitative analysis,
210 and provides indications if the material has been heated or not [4], and efficiently produces
211 semi-quantitative estimations of absorbed dose (apparent absorbed dose) for luminescence
212 dating [4, 25, 38, 39, 41]. In the semi-quantitative luminescence protocol, signals that
213 resulted from a single regenerative dose in the quasi-linear region of the sample's dose
214 response are used. The extrapolation of the quasi-linear calibration dose response would
215 tend to overestimate the signal that resulted from doses in the range of 10–200 Gy, in which
216 the effects of saturation in the dose response. So, to allow the comparison between all
217 results, the apparent absorbed doses obtained were estimated by using a common saturating
218 exponential dose response characteristic (DRC). It was defined by using the average of the
219 standardised post- IR OSL responses to 50 sβ, with test dose of 10 sβ used in all analyses.
220 The DRC is described by a single saturating exponential function, $I = I_{\infty}(1 - \exp(-D/D))$
221 using a signal at saturation (I_{∞}) equal to the average dose of signal saturation (D) [42]. For

222 each sample, the average of the five apparent absorbed dose and the respective uncertainty
 223 was calculated.

224

225 **Table 1** Sequence for semi-quantitative luminescence protocol, using a Riso TL/OSL
 226 automatic reader with a $^{90}\text{Sr}/^{90}\text{Y}$ beta. Beta irradiators giving $0,0842 (\pm 0,0009) \text{ Gys}^{-1}$.

Sequence	Two cycles	
	Natural	After irradiation (5 Gy)
Preheat TL	240 °C, 5 °C/s	
IRSL	125 s, 50 °C	
OSL	125 s, 125 °C	
Test Dose	1 Gy	
Preheat TL	160 °C, 5 °C/s	
IRSL	125 s, 50 °C	
OSL	125 s, 125 °C	
TL	500 °C, 5 °C/s	

227

228 The application of quantitative luminescence protocols to attain the proposed objectives is
 229 mainly supported by the known response of quartz grains to the thermal and optical
 230 stimulation [43]. Those protocols can provide information about heating temperatures and
 231 detect the amount of time elapsed from the last heating. The latter is correlated with the
 232 emitted light intensity (Equivalent Dose, D_e) taking into account the dose rate (D_r) in the
 233 studied material and its environment and enables to obtain the luminescence age (D_e/D_r)
 234 [43]. For the chronological assessment, the luminescence approaches include the
 235 quantitative analyses to obtain the absorbed dose. Before these analyses, the quartz purity
 236 check [44] and the dose recovery test [45] were performed. For the quantitative
 237 determination of the absorbed dose, a SAR-OSL protocol with an internal pre-heat test was
 238 applied to the enriched coarse quartz grains fraction [46]. Twenty-four aliquots were
 239 measured and the sequence of regenerative calibration doses is shown on Table 2.

240 **Table 2** Calibration doses (in seconds) used in SAR-OSL sequences for luminescence
 241 dating of heated material collected at La Turquesa prehistoric mine (sample MT1_1, shaft
 242 L2). OSL was measured at 125 °C for 125 s. Beta irradiators giving 0,120 (\pm 0,002) Gys⁻¹.
 243 The sequence includes a pre-heat test with temperatures between 180 °C and 280 °C and
 244 the cut heat temperature was 160 °C.

Sequence	Time of irradiation (s)	Aliquots	Pre-heat temperature (°C)
Natural	-	1-4	180
β	40	5-8	200
Z	0		
$\beta/4$	10	9-12	220
$\beta/2$	20		
2 β	80	13-16	240
4 β	160		
Zero (R)	0	17-20	260
β (R)	40		
β (IR)	40	21-24	280
β test	7		

245 where R indicates a repeat point and IR indicates a repeat point where OSL response was
 246 measured following infrared exposure to test the presence of other minerals than quartz.

247

248 Signals were obtained by subtracting the average count rate in the last 5 s of measurement
 249 from that in the first 5 s, which included the majority of the rapidly decaying OSL. Signals
 250 normalized to subsequent test dose responses were fitted with linear curves, and the
 251 absorbed dose was interpolated. Based on Luminescence Analyst software [47], results
 252 were accepted when: (i) the relative uncertainty of the natural test dose signal σT_n was <
 253 10 %; (ii) the recycling ratio was consistent with unity at 2σ ; (iii) the OSL IRSL depletion
 254 ratio [44] was consistent with unity at 2σ ; and (iv) the sensitivity corrected recuperation
 255 signal (i.e., the OSL signal in response to a zero Gy regenerative dose) was consistent with
 256 zero at 2σ . The accepted results were statistically analysed to estimate the absorbed dose
 257 for the sample using the robust mean and the respective uncertainty calculated by Robust
 258 Statistics V1.0 [48].

259 Dose rate estimation was obtained combining cosmic, beta, and gamma dose rates. The
260 cosmic dose rate was calculated considering the density of the studied materials [49, 50],
261 and attenuation factors were applied [51]. The evaluation of the material dose rate was
262 made considering the chemical content of K, Rb, Th and U, obtained by INAA. The
263 environment dose rate was determined in situ measurements using a field gamma-ray
264 spectrometer (FGS) at each sampling location, using a 3''x 3'' NaI probe with an HPI
265 Rainbow MCA. Stripped counts in the windows 1380–1530 keV, 1690–1840 keV, and
266 2550–2760 keV (designed to obtain signals dominated by ^{40}K , ^{214}Bi and ^{208}Tl respectively),
267 were calibrated relative to previous measurements in the Oxford and the Gif-sur-Yvette
268 blocks [52, 53], to obtain apparent parent element concentrations, assuming equilibrium in
269 the ^{232}Th and ^{238}U series. The estimation of beta and gamma radiation was obtained from
270 elemental concentrations of K, Rb, Th and U using conversion factors [51] and was
271 corrected for water content [54], assuming 5% of water content. For the dose rate
272 estimation, 83% of beta dose obtained from INAA results and 21% of gamma dose from
273 INAA results added to 79% from FGS results were considered.

274

275 **Results and discussion**

276

277 **Compositional studies**

278 In order to achieve a more detailed characterization of La Turquesa mine, a compositional
279 study was performed to complement the luminescence analysis. In this way, the
280 mineralogical assemblage [22] and the chemical composition of the two mining shafts and
281 geological background was made. The XRD analyses performed showed that quartz is the
282 main mineral in all samples. Phyllosilicates, particularly micas, and traces of hematite and
283 cuprite (Table 3) occur. Azurite was detected in trace amounts in the Cu vein and on
284 samples MT2_1 and MT2_2, and the highest proportion of phyllosilicates was found in the
285 sediment. All these results are in accordance with the mineralogical associations obtained
286 earlier for the mineralised zones and the host rock [23] of this area. Despite the high
287 temperatures, which can promote the production of new formed minerals [32, 55–57], no
288 mineral phases resulting from this process were observed [22]. However, in La Turquesa
289 mine “fire-setting” cannot be excluded, and was previously discussed [22].

290 The chemical results obtained by INAA and XRF for La Turquesa mine samples show that
291 all samples are mainly composed by SiO₂ (Table 3), which is in accordance with the
292 mineralogical assemblage found. Some chemical variations are observed in the studied
293 samples: (i) despite the low amounts of CuO in samples, the higher contents were detected
294 in the samples collected nearest to the copper vein, as expected, in each shaft (MT1_3,
295 MT1_4, MT2_2, and MT2_3) particularly in sample MT2_2, where an intense blue colour
296 (Fig.) was observed during the sampling process, nevertheless only traces of azurite and
297 cuprite were identified by XRD in these samples; (ii) the highest contents of Na₂O, MgO,
298 Al₂O₃, K₂O, TiO₂, Rb, Cs, Ce and Th were detected in the sediment (MT2_1) collected at
299 the shaft L3, where the higher proportions of phyllosilicates were detected; (iii) the lowest
300 contents of P₂O₅, CaO, V₂O₅, Fe₂O₃, CuO, Cr, Mo, Sb, heavy rare earth elements (HREE)
301 and U, and the highest content of Si₂O occur on the samples of geological background
302 (MT3 and MT4), in accordance with the higher amounts of quartz; and (iv) the highest
303 contents of P₂O₅, CaO, MnO, and Co were found in sample MT1_4. Higher contents of
304 rare earth elements (REE) are found on shaft L3, except for sample MT2_2. Samples MT3

305 and MT4 show positive Ce anomalies and, in general, L2 samples show lower fractionation
306 of REE.

307 In general, the high proportions of quartz present in samples may difficult the identification
308 of other mineral phases, existing in smaller amounts, and which may incorporate some of
309 the chemical elements such as Co, Mn or As. It should be noted that other techniques should
310 be applied to identify these mineral phases that could include carbonates, iron oxy-
311 hydroxides or heavy minerals.

312 Despite the heterogeneity observed in the chemical composition of the samples collected
313 in the shafts, a cluster analysis using chemical elements as variables, and unweighted pair-
314 group average rule and the Pearson correlation coefficient, suggests the existence of three
315 clusters. One of the clusters comprises the rock samples (MT3 and MT4) and the sediment
316 (MT2_1) suggesting that this sample collected on the shaft L3 may be derived from the
317 weathering of the bedrock surrounding. It should be mention that this sediment was
318 deposited at the shaft L3 after the last mining activities.

319

320

321 **Table 3** Chemical composition obtained by INAA and XRF; semi-quantification of
 322 mineralogical assemblage obtained by XRD for the samples collected at shafts L2 and L3
 323 from La Turquesa prehistoric mine (nd – not detected; * - including micas; traces - < 5%).

	L2				L3				Bedrock		Cu vein
	MT1_1	MT1_2	MT1_3	MT1_4	MT2_1	MT2_2	MT2_3	MT2_4	MT3	MT4	MT5
Na₂O	0.020	0.010	0.010	0.010	0.090	0.010	0.010	0.010	0.010	0.020	0.010
MgO	0.080	0.040	0.080	0.050	0.290	0.010	0.070	0.150	0.070	0.140	0.110
Al₂O₃	1.70	1.19	2.34	1.86	5.43	1.39	2.82	4.41	1.61	2.63	3.59
SiO₂	94.3	95.6	91.5	91.7	88.2	94.1	89.6	83.9	97.4	94.9	86.1
P₂O₅	0.100	0.120	0.280	1.060	0.200	0.230	0.760	0.510	0.020	0.040	0.370
K₂O	0.460	0.300	0.520	0.400	1.28	0.320	0.620	1.00	0.490	0.690	0.860
CaO	0.070	0.060	0.080	1.07	0.230	0.180	0.340	0.110	0.010	0.030	0.110
TiO₂	0.060	0.040	0.090	0.060	0.340	0.050	0.100	0.120	0.050	0.120	0.120
V₂O₅	0.081	0.088	0.097	0.022	0.027	0.036	0.115	0.058	0.003	0.008	0.068
MnO	0.003	0.002	0.002	0.363	0.066	0.003	0.003	nd	0.002	0.002	0.002
Fe₂O₃(Total)	2.23	1.01	2.99	1.24	1.59	0.730	3.03	5.95	0.390	0.940	5.76
CuO	0.183	0.197	0.679	0.792	0.115	1.32	0.675	0.393	0.028	0.022	0.329
Sc	2.60	1.80	3.50	3.30	7.30	1.90	3.80	8.90	2.40	3.10	4.90
Cr	90.0	85.0	50.0	18.0	37.0	29.0	109	115	12.0	15.0	62.0
Co	7.00	5.00	7.00	733	39.0	5.00	12.0	23.0	7.00	4.00	19.0
As	111	76.1	216	332	196	127	756	942	49.1	106	112
Br	1.10	1.20	0.600	nd	1.30	0.900	nd	4.60	nd	1.00	nd
Rb	Nd	18.0	32.0	nd	55.0	nd	30.0	22.0	23.0	18.0	51.0
Mo	31.0	17.0	42.0	32.0	8.00	14.0	54.0	218	nd	1.00	60.0
Sb	3.20	1.90	8.90	3.80	4.30	4.00	24.9	55.0	1.00	1.90	3.90
Cs	1.00	Nd	Nd	1.00	3.00	nd	nd	nd	2.00	2.00	3.00
Ba	160	170	140	150	380	nd	550	130	210	260	200
La	4.20	4.50	15.0	12.0	32.0	9.90	30.6	51.0	8.10	10.8	18.9
Ce	9.00	9.00	28.0	28.0	59.0	18.0	44.0	57.0	19.0	28.0	34.0
Nd	6.00	7.00	28.0	16.0	21.0	12.0	35.0	28.0	9.00	10.0	31.0
Sm	0.900	0.900	4.00	2.70	4.00	1.60	6.60	4.20	1.10	1.50	6.10
Eu	0.400	0.400	1.30	1.50	1.20	0.600	2.30	1.60	0.300	0.400	2.40
Tb	0.050	0.050	1.40	0.050	0.600	0.050	1.50	0.050	0.050	0.050	1.80
Yb	0.900	0.900	2.00	1.30	1.90	0.900	4.30	2.20	0.400	0.900	2.50
Lu	0.240	0.230	0.480	0.410	0.430	0.220	0.840	0.600	0.070	0.130	0.540
Th	1.10	0.800	1.80	2.30	5.20	1.30	2.50	4.40	1.30	2.80	2.60
U	9.40	9.70	20.5	19.0	6.00	8.10	26.7	30.4	1.30	0.900	22.0
Quartz	87	94	90	92	76	96	94	85	94	91	87
Phyllosilicates	9 *	Traces	8 *	5 *	21 *	Traces*	6 *	12 *	6	6 *	9 *
Hematite	Traces	Traces	Nd	Traces	Traces	Traces	Traces	Traces	nd	nd	Traces
Cuprite	Traces	Traces	Traces	Traces	Traces	nd	nd	Traces	nd	Traces	Traces
Azurite	nd	Nd	Nd	nd	Traces	Traces	nd	nd	nd	nd	Traces

324

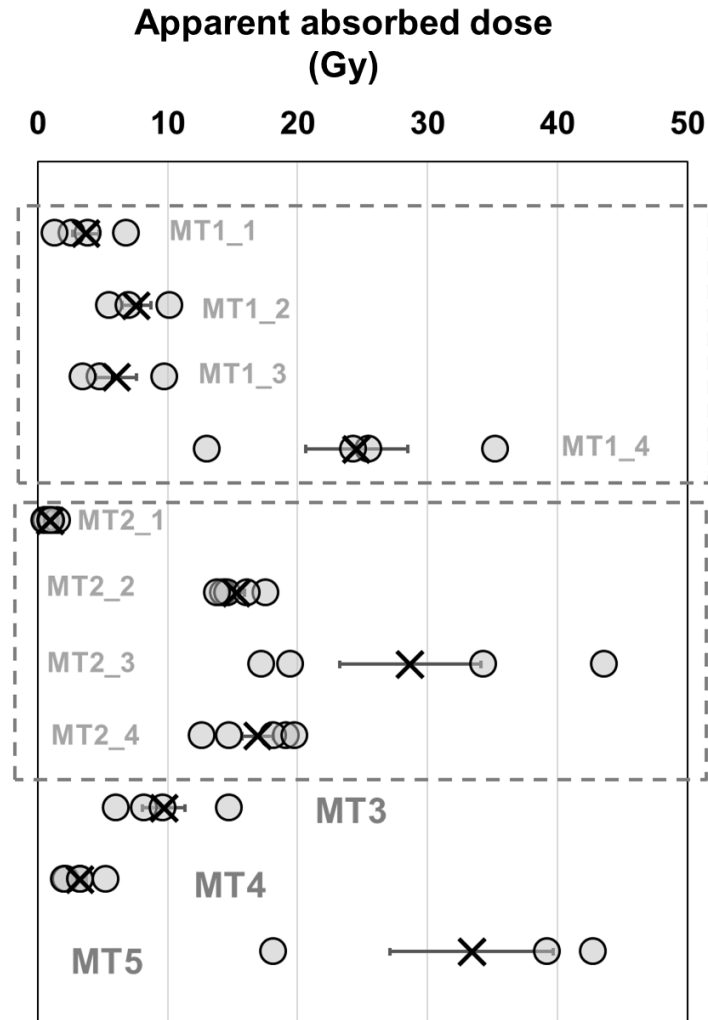
325 **Luminescence studies**

326 The first luminescence measurements performed in La Turquesa mine [22] were used to
327 identify eventual heating of coarse quartz grains extracted from rock fragments and
328 sediment. The results previously obtained pointed out that in shaft L2, the TLn signals of
329 the enriched quartz coarse grains fraction have a higher intensity than those of the TLr. The
330 same behaviour was found for the shaft L3, indicating that the analysed quartz retains most
331 of the unchanged geological signal. The detailed description of these luminescence
332 measurements were reported in the previous work[22], and the Semi-quantitative
333 luminescence protocol applied demonstrates the heating of some analysed samples,
334 corroborating the results obtained by TL protocol [22]. In addition, this semi-quantitative
335 protocol was used to plan further luminescence approaches, by evaluating the behaviour of
336 quartz grains to regenerative protocols for the determination of the absorbed dose. In
337 general, quartz grains have slightly sensitivity changes when natural signals are compared
338 with regenerative signals (after irradiation with 5 Gy). In this work, the most evident
339 sensitivity changes were observed for samples MT2_1 and MT3, indicating that the quartz
340 of these samples is not the most suitable one for the application of the luminescence
341 regenerative protocols to determine the absorbed dose. The ratio between the absorbed
342 doses obtained by IRSL and OSL signals, using the INIT protocol, was less than 1 for most
343 of the samples allowing to infer about the purity of the analysed quartz: IRSL/OSL <1
344 point to low feldspars contamination. The OSL signals obtained using the semi-quantitative
345 protocol, were also useful to detect the eventual heating of coarse quartz grains extracted
346 from analysed samples, as well as to estimate the average of the apparent absorbed dose
347 (Fig. 3).

348 Regarding the quartz extracted from the sediment used as reference for the luminescence
349 signal boundary of last mining activity (MT2_1), it has the lowest apparent absorbed dose
350 (about 1 Gy). This means that in this sample, the geological signal was bleached by light
351 and/or heat exposure. After the bleach of the geological signal, the absorbed dose obtained
352 reflects the time since the MT2_1 sediment was deposited in shaft L3, probably
353 corresponding to the end of last mining activities. Regarding the quartz grains extracted
354 from the rock fragments used as reference for the luminescence signal boundary of
355 geological signal (MT3 and MT4), they have low apparent absorbed doses, especially the

356 sample MT4 with 3 Gy. These low doses are probably a consequence of the loss of
357 geological signal during recently mining activities. The sample collected in the non-
358 exploited copper vein (MT5) and used as reference for the luminescence signal boundary
359 of geological signal has the highest apparent absorbed dose preserving the geological
360 signal. For the rock fragments MT1_4 (shaft L2), MT2_2, MT2_3 and MT2_4 (shaft L3)
361 high values of apparent absorbed dose were obtained, 15 - 29 Gy, pointing to the absence
362 of heating and indicating that the analysed quartz retains most of the unbleached geological
363 signal. For the rock fragments MT1_1, MT1_2 and MT1_3, collected in shaft L2, lower
364 apparent absorbed doses were obtained, ranging from 4 Gy to 8 Gy, suggesting that the
365 quartz grains extracted from these samples were probably bleached by the “fire-setting”
366 procedure. Despite the lower values obtained for these three samples, an incomplete
367 bleaching (partial removal of the natural geological signal) was observed, due to the
368 heterogeneous heating conditions associated to this mining procedure. Thus, an
369 overestimation and a spread of results of the apparent absorbed dose occur. The lower
370 apparent absorbed dose (about 4 Gy) obtained for sample MT1_1 indicates that quartz from
371 this sample must have had more homogeneous heating conditions. In this case, the sample
372 MT1_1 seems to have better bleaching conditions, and can be considered as a
373 representative sample of the heating event related with “fire-setting” in the pre-historic
374 period.

375 Comparing the two approaches, TL and semi-quantitative protocols, the use of “fire-
376 setting” techniques to copper ore extraction in the prehistoric seems to be confirmed, being
377 the semi-quantitative protocol a better option since it enables to evaluate diverse
378 luminescence signals (IRSL, OSL, TL) using low amount of material, and in a faster way.
379



380

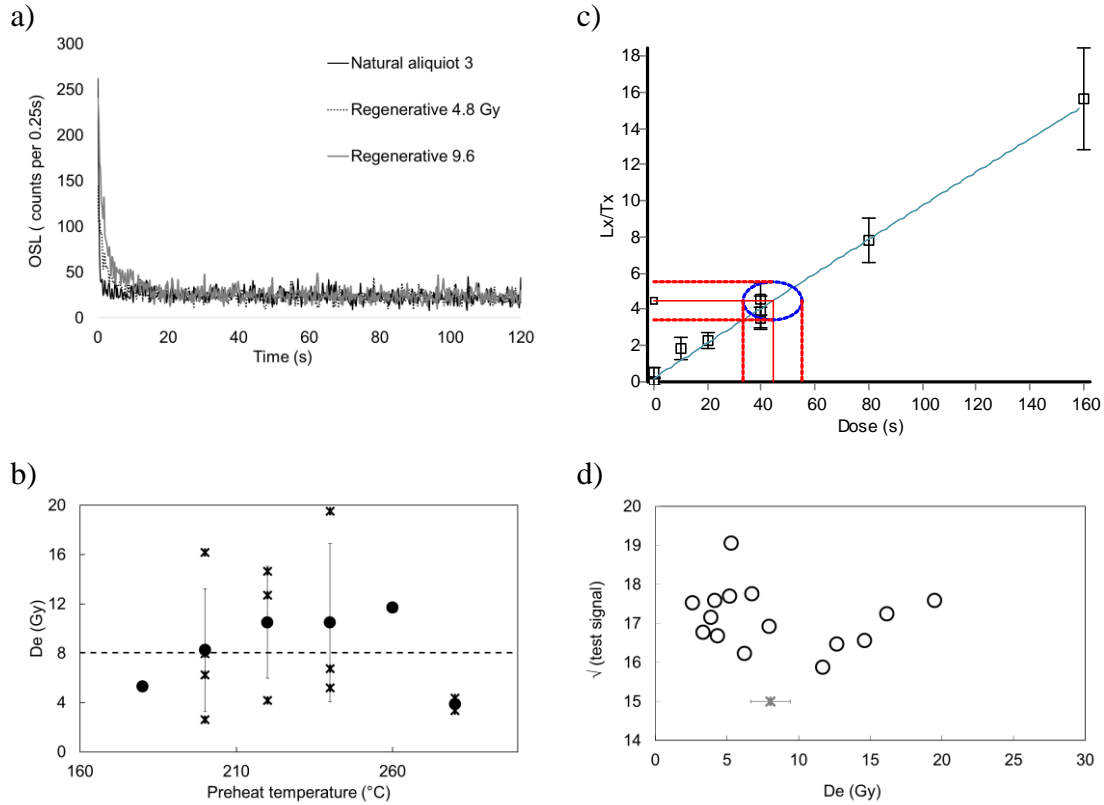
381 **Fig. 3** Apparent absorbed dose, obtained by applying the INIT luminescence protocol to
 382 enriched quartz coarse grains fraction extracted from samples collected at La Turquesa
 383 mine (Cornudella de Montsant, Catalonia, Spain). The absorbed dose was obtained
 384 considering the OSL signals of five aliquots for each sample. The average and the
 385 respective uncertainty are highlighted (X)

386

387 Considering that sample MT1_1 had better bleaching conditions, this sample was the only
 388 one selected to further luminescence protocols, performing the quartz purity and the dose
 389 recovery tests. The quartz purity test shows that OSL IR depletion ratio of the quartz grains
 390 from MT1_1 was smaller than 10 % and the dose-recovery test shows that the mean of
 391 dose recovery ratio (measured/given dose) for three aliquots was 1.06 ± 0.02 , pointing to
 392 the applicability of SAR-OSL protocol to determine absorbed dose in this sample.

393 The quantitative analyses performed by SAR-OSL protocol on sample MT1_1, only 15 of
394 the 24 aliquots have acceptable results. The measured material shows a recycling ratio ~ 1 ,
395 as expected based on quartz purity test. The OSL signal is dominated by the fast
396 component, which is usually considered better for quartz OSL dating (Fig. 4a). No
397 consistent effect of preheat temperature in the De was observed, and there is a wide
398 dispersion of values for each temperature tested (Fig. 4b). For each aliquot, the De obtained
399 shows high uncertainties (an example in Fig. 4c) and the obtained robust mean using the
400 15 accepted values was 8 ± 1 Gy (Fig. 4d). The over dispersion of values and the
401 uncertainties observed in each aliquot might be a consequence of the heterogeneous heating
402 processes that produces an incomplete bleach. Some grains may have been exposed to
403 sufficiently high temperatures to completely empty the latent OSL signals, whereas other
404 grains still carry a residual OSL geological signal. The existing residual remains of the
405 copper mining activities may explain the observed heterogeneity of the bleaching processes
406 of MT1_1 material. Thus, the determination of the equivalent dose in incompletely
407 bleached samples using multi-grain aliquots can lead to significant dose overestimation.

408



409 **Fig. 4** SAR-OSL results for quartz from sample MT1_1 collected at La Turquesa mine
 410 (Cornudella de Montsant, Catalonia, Spain): a) OSL natural and regenerative curves for
 411 aliquot 3; b) De values as a function of preheat temperature (mean values of each
 412 temperature - full marks); c) example of sensitive corrected OSL (L_x/T_x) as a function of
 413 regenerative doses for aliquot 13 at preheat 240 °C; and d) Square root of tests signal as a
 414 function of De (robust mean - cross mark)

415

416 Considering the K, Rb, Th and U contents obtained by INAA and FGS (Table 4), as well
 417 as the estimated dose rate of sample MT1_1 (2.8 ± 0.1 Gy/ka), and the absorbed dose
 418 obtained by SAR-OSL (8 ± 1 Gy), the luminescence age obtained for this sample is $2.8 \pm$
 419 0.4 ka. This date indicates a chronological framework between 1400 and 600 BC, that is, a
 420 span of 800 years.

421

422

423

424 **Table 4** Chemical elements content obtained by INAA and FGS for sample MT1_1
 425 collected at shaft L2 from La Turquesa prehistoric mine (Cornudella de Montsant,
 426 Catalonia, Spain).

		INAA	FGS
K	(%)	0.46	0.402
	±	0.02	0.008
Rb	(mg/kg)	14.0	nd
	±	0.7	nd
U	(mg/kg)	9.4	8.3
	±	0.5	0.8
Th	(mg/kg)	1.10	2.3
	±	0.06	0.2

427 (nd – not determined)

428

429 The historical-archaeological interpretation of the luminescence age here obtained
 430 confirms the prehistoric character of the mining work documented during the
 431 archaeological excavations. This fact is supported by the unequivocally prehistoric
 432 attribution of the assemblage of macrolithic mining tools recovered [58]. As previously
 433 mentioned, the lead isotope analysis also showed that probably the mine was exploited in
 434 the Late Chalcolithic (2800-2300 cal BC), due to the coincidence of the isotopic signature
 435 of the mine with a copper awl of Coveta de l'Heura (Ulldemolins). The set of mining tools
 436 more elaborated and with hafting devices to be handled, as well as the isotopic coincidence
 437 with the smelting vessel of the Balma del Duc (Montblanc), point to an exploitation in the
 438 Early-Middle Bronze Age (2300-1350/1300 cal BC) [24]. Regarding the radiocarbon
 439 dating [21] of the shaft L1, it is not possible to know if there was mining exploitation in
 440 medieval times, although there is no doubt that during this period there was a filling phase.
 441 The luminescence ages obtained for shaft L2 may indicate an exploitation phase at the end
 442 of the Middle Bronze Age, or in the Late Bronze Age (3.0 ± 0.4 ka, 1.0 ± 0.4 ka), or already
 443 in the Iron Age. Considering the archaeological evidence, this late age may be a
 444 consequence of the uncompleted bleach of the quartz grains observed, resulting in a higher
 445 range of the luminescence age. This fact is also supported by the archaeological
 446 investigations carried out on settlements, and on circulation of metals in Priorat County,
 447 from the year 2000 until now. This revealed that during the Iron Age, copper was mainly
 448 imported from the south of the Iberian Peninsula (the mining basin of Linares, Jaén), and

449 to a lesser extent, from the southeast [59, 60], and that local copper comes from the Molar-
450 Bellmunt-Falset basin (south of the country).

451 Finally, it is important to highlight that the luminescence age of the sample MT1_1
452 collected at shaft L2 is subsequent to the shaft L1. From a stratigraphic point of view and
453 taking into account the way of operating in ancient mining, most probably the mining shafts
454 L2 and L3 were opened after the shaft L1. As a result, the new luminescence ages provide
455 an *ante quem* date for it.

456

457 **Conclusions**

458 The compositional studies enabled a more detailed compositional characterization of the
459 mined Cu-vein materials and geological background at La Turquesa mine. Despite the
460 heterogeneity in samples composition, a relation between bedrock samples and the
461 sediment was found.

462 The luminescence protocols approach used in this work, particularly the semi-quantitative
463 protocol, has more advantages than the TL protocol, as it needs lower amount of material
464 and measurement time, it enables the estimation of the absorbed dose, as well as the study
465 of multiple luminescence signals (TL, IRSL and OSL). This prior comprehensive
466 luminescence study of samples enables to design dating protocols in a more suitable way.

467 The selection of samples as luminescence boundaries for both geological and last mining
468 activity signals reveals to be a good strategy for the interpretation of the luminescence
469 results, and better understand the luminescence properties of the analysed materials,
470 enabling a better establishment of the chronological framework of the studied contexts.

471 This work demonstrates the suitability of luminescence for identifying “fire-setting”
472 techniques in mining contexts and evaluate the absolute dating properties of the samples.

473 The results obtained from luminescence measurements allowed inferring that sample
474 MT1_1 collected at shaft L2 was exposed to “fire-setting” conditions, as shown by the
475 lower apparent absorbed dose obtained. The luminescence age of this sample points to
476 mining exploitation at La Turquesa mine during the Middle/Late Bronze Age.

477 Considering that the character of mining often leads to destruction of the archaeological
478 record making difficult to date the contexts and lithic tools, the used methodology in this

479 work, by dating through luminescence, is a valuable contribution to more accurate absolute
480 dating of ancient mining activities with “fire-setting” evidence.

481

482 **Acknowledgements**

483 Portuguese team gratefully acknowledge the FCT (Portuguese Science and Technology
484 Foundation) support through the UID/Multi/04349/2013 and UID/Multi/04349/20 (including a
485 post-doctoral grant BL 36/2016_IST-ID of the first author in the C2TN) and post-doctoral grant
486 SFRH/BPD/114986/2016 of the first author. Archaeometric and archaeological research has been
487 possible thanks to various projects financed by the Autonomous Government of Catalonia and the
488 Government of Spain: *The protohistoric archaeological site of El Calvari del Molar and the*
489 *mining-metallurgical area of Molar-Bellmunt-Falset (2000-2012)* and *Mining and Metallurgy in*
490 *southern Catalonia: from Prehistory to the Mediaeval Period, 2014-2017* (Department of Culture,
491 Government of Catalonia); *The mining-metallurgical area of Molar-Bellmunt-Falset in*
492 *Protohistory* (Ministry of Science and Innovation, HUM2004-04861-C03-01); *The mining-*
493 *metallurgical area of Molar-Bellmunt-Falset in Protohistory: a comparison of hypotheses*
494 *(Ministry of Science and Innovation, HAR2007-65725-C03-01)*; *Social, technological and*
495 *economic processes in the exploitation of mineral resources in the Priorat (Catalonia): a*
496 *diachronic view* (Ministry of Science and Innovation, HAR2010-21105-C02-01) and *Mineral-*
497 *metallic resources, trade and commerce in the prehistory and protohistory of the Iberian Peninsula*
498 *(Catalonia and the north of the Valencian Country)* (Ministry of the Economy and
499 Competitiveness, HAR2014-54012-P). The study of the structure and mineralogy of the mine was
500 carried out within the framework of the Consolidated Group of Mineral Resources 2014SGR 1661
501 of the Government of Catalonia. The archaeometry of minerals and metals was made possible by
502 the technical and human support provided by the SGIker of the University of the Basque Country
503 (EHU) and European funding (ERDF and ESF).

504

505 **References**

- 506 1. Craddock PT (1992) A short history of firesetting. *Endeavour* 16:145–150.
507 [https://doi.org/10.1016/0160-9327\(92\)90074-Y](https://doi.org/10.1016/0160-9327(92)90074-Y)
- 508 2. Weisgerber G, Willies L (2000) The use of fire in prehistoric and ancient mining-
509 firesetting in La pyrotechnologie à ses débuts. *Evolution des premières industries*

- 510 faisant usage du feu. 131-149. *Paléorient* 26:131–149
- 511 3. Ambert P (2002) Utilisation préhistorique de la technique minière d’abattage au
512 feu dans le district cuprifère de Cabrières (Hérault). *C. R. Palevol* 1:711 – 716
- 513 4. Odriozola CP, Villalobos García R, Burbidge CI, et al (2016) Distribution and
514 chronological framework for Iberian variscite mining and consumption at Pico
515 Centeno, Encinasola, Spain. *Quat Res (United States)* 85:159–176.
516 <https://doi.org/10.1016/j.yqres.2015.11.010>
- 517 5. Pichler T, Nicolussi K, Goldenberg G, et al (2013) Charcoal from a prehistoric
518 copper mine in the Austrian Alps: dendrochronological and dendrological data,
519 demand for wood and forest utilisation. *J Archaeol Sci* 40:992–1002.
520 <https://doi.org/10.1016/j.jas.2012.09.008>
- 521 6. Py V, Durand A, Ancel B (2013) Anthracological analysis of fuel wood used for
522 firesetting in medieval metallic mines of the Faravel district (southern French
523 Alps). *J Archaeol Sci* 40:3878–3889. <https://doi.org/10.1016/j.jas.2013.05.006>
- 524 7. Shindo L, Py-Saragaglia V, Ancel B, et al (2019) New insights on the chronology
525 of medieval mining activity in the small polymetallic district of Faravel (Massif
526 des Écrins, Southern French Alps) derived from dendrochronological and
527 archaeological approaches. *J Archaeol Sci Reports* 23:451–463.
528 <https://doi.org/10.1016/J.JASREP.2018.11.008>
- 529 8. Py V, Ancel B (2006) Archaeological experiments in fire-setting: protocol, fuel
530 and anthracological approach. *Charcoal analysis: new analytical tools and methods*
531 for archaeology. In: *Papers from the table-ronde held in Basel, 14-15 octobre*
532 2004, Volume: BAR International Series S
- 533 9. Ancel B, Py V (2008) L’abattage par le feu: une technique minière ancestrale.
534 *Archéopages* 22:34–41
- 535 10. Py-Saragaglia V, Cunill Artigas R, Métailié JP, et al (2017) Late Holocene history
536 of woodland dynamics and wood use in an ancient mining area of the Pyrenees
537 (Ariège, France). *Quat Int* 458:141–157.
538 <https://doi.org/10.1016/j.quaint.2017.01.012>
- 539 11. De Jesus P, Dardeniz G (2015) Archaeological and geological concepts on the
540 topic of ancient mining. *Bull Miner Res Explor* 151:231–246.

- 541 <https://doi.org/10.19111/bmre.54281>
- 542 12. Poggiali F, Buonicontri MP, D’Auria A, et al (2017) Wood selection for
543 firesetting: First data from the Neolithic cinnabar mine of Spacasso (South
544 Tuscany, Italy). *Quat Int* 458:134–140.
545 <https://doi.org/doi.org/10.1016/j.quaint.2017.06.028>
- 546 13. Stöllner TR (2014) *Methods of Mining Archaeology (Montanarchäologie)*.
547 *Archaeometall Glob Perspect* 133–159. [https://doi.org/10.1007/978-1-4614-9017-](https://doi.org/10.1007/978-1-4614-9017-3_7)
548 [3_7](https://doi.org/10.1007/978-1-4614-9017-3_7)
- 549 14. Castaing J, Mille B, Zink A, et al (2005) L’abattage préhistorique au feu dans le
550 district minier de Cabrieres (Hérault): évidences par thermoluminescence (TL). In
551 *La premiere métallurgie en France et dans les pays limitrophes. Mémoire XXXVII*
552 *la Société Préhistorique Française* 53–62 53–62
- 553 15. Rapp G (Rip), Balescu S, Lamothe M (1999) The Identification of Granitic Fire-
554 Cracked Rocks Using Luminescence of Alkali Feldspars. *Am Antiq* 64:71–78.
555 <https://doi.org/10.2307/2694346>
- 556 16. Eskola K. O, Okkonen J, Jungner H (2003) Luminescence dating of a coastal
557 Stone Age dwelling place in Northern Finland. In: *Quaternary Science Reviews*.
558 Pergamon, pp 1287–1290
- 559 17. Armitage SJ, King GE (2013) Optically stimulated luminescence dating of hearths
560 from the Fazzan Basin, Libya: A tool for determining the timing and pattern of
561 Holocene occupation of the Sahara. *Quat Geochronol* 15:88–97.
562 <https://doi.org/10.1016/J.QUAGEO.2012.10.002>
- 563 18. Richter D, Angelucci DE, Dias MI, et al (2014) Heated flint TL-dating for Gruta
564 da Oliveira (Portugal): dosimetric challenges and comparison of chronometric
565 data. *J Archaeol Sci* 41:705–715. <https://doi.org/10.1016/j.jas.2013.09.021>
- 566 19. Burbidge CI, Trindade MJ, Dias MI, et al (2014) Luminescence dating and
567 associated analyses in transition landscapes of the Alto Ribatejo, Central Portugal.
568 *Quat Geochronol* 20:65–77. <https://doi.org/10.1016/j.quageo.2013.11.002>
- 569 20. Sanjurjo-Sánchez J, Gomez-Heras M, Fort R, et al (2016) Dating fires and
570 estimating the temperature attained on stone surfaces. The case of Ciudad de
571 Vascos (Spain). *Microchem J* 127:247–255.

- 572 <https://doi.org/10.1016/J.MICROC.2016.03.017>
- 573 21. Rafel Fontanals N, Hunt MA, Soriano I, Delgado-Raack S (2018) Prehistoric
574 copper mining in the northeast of the Iberian Peninsula: La Turquesa or Mas de les
575 Moreres Mine (Cornudella de Montsant, Tarragona, Spain). *Revista d'Arqueologia*
576 *de Ponent*, Número extra 3, Universitat de Lleida, Lleida
- 577 22. Rodrigues AL, Cardoso G, Dias MI, et al (2018) Thermoluminescence as a tool for
578 identifying archaeological “firesetting” evidence in at La Turquesa mine in
579 Cornudella de Montsant, Catalonia. In: Rafel Fontanals N, Hunt MA, Soriano I,
580 Delgado-Raack S (eds) Prehistoric copper mining in the northeast of the Iberian
581 Peninsula: La Turquesa or Mas de les Moreres Mine (Cornudella de Montsant,
582 Tarragona, Spain). *Revista d'Arqueologia de Ponent*, Número extra 3, Universitat
583 de Lleida, Lleida, pp 33–40
- 584 23. Andreazini A, Melgarejo JCC, Rafel Fontanals N, et al (2018) The structure and
585 mineralogy of the mine. In: Rafel Fontanals N, Hunt MA, Soriano I, Delgado-
586 Raack S (eds) Prehistoric copper mining in the northeast of the Iberian Peninsula:
587 La Turquesa or Mas de les Moreres Mine (Cornudella de Montsant, Tarragona,
588 Spain)., *Revista d'Arqueologia de Ponent*, Número extra 3, Universitat
589 de Lleida, Lleida., Lleida, p 169
- 590 24. Montero-Ruiz I (2018) The archaeometallurgical perspective. In: Rafel Fontanals
591 N, Hunt MA, Soriano I, Delgado-Raack S (eds) Prehistoric copper mining in the
592 northeast of the Iberian Peninsula: La Turquesa or Mas de les Moreres Mine
593 (Cornudella de Montsant, Tarragona, Spain). *Revista d'Arqueologia de Ponent*,
594 Número extra 3, Universitat de Lleida, Lleida., Lleida, pp 63–72
- 595 25. Rodrigues AL, Dias MI, Valera AC, et al (2019) Geochemistry, luminescence and
596 innovative dose rate determination of a Chalcolithic calcite-rich negative feature. *J*
597 *Archaeol Sci Reports* 26:101887. <https://doi.org/10.1016/j.jasrep.2019.101887>
- 598 26. Brindley GW (1955) Identification of clays mineralogy by X-Ray Diffraction
599 analysis. *First Natl Conf Clays Clay Technol Bull.* 169:319–328.
600 <https://doi.org/10.1346/CCMN.1952.0010116>
- 601 27. Biscaye PE (1965) Mineralogy and sedimentation of recent deep-sea clay in the
602 Atlantic Ocean and adjacent seas and oceans. *Geol Soc Am Bull* 76:803–832

- 603 28. Martin-Pozas JM. (1968) El análisis mineralógico cuantitativo de los filosilicatos
604 de la arcilla por difracción de rayos X. University of Granada, Spain
- 605 29. Rocha FJFT (1993) Argilas aplicadas a estudos litoestratigráficos e
606 paleoambientais na bacia sedimentar de Aveiro. University of Aveiro, Portugal
- 607 30. Schultz LG (1964) Quantitative interpretation of mineralogical composition X-ray
608 and chemical data for the Pierre Shale. U.S. Geol Surv Prof Pap 391:1–31
- 609 31. Trindade MJ, Dias MI, Rocha F, et al (2011) Bromine volatilization during firing
610 of calcareous and non-calcareous clays: Archaeometric implications. *Appl Clay*
611 *Sci* 53:489–499. <https://doi.org/10.1016/j.clay.2010.07.001>
- 612 32. Trindade MJ, Dias MI, Coroado J, Rocha F (2009) Mineralogical transformations
613 of calcareous rich clays with firing: A comparative study between calcite and
614 dolomite rich clays from Algarve, Portugal. *Appl Clay Sci* 42:345–355.
615 <https://doi.org/10.1016/j.clay.2008.02.008>
- 616 33. Rodrigues AL, Dias MI, Prudêncio MI, et al (2019) Paleoenvironmental
617 considerations based on geochemistry and mineralogy of a Miocene lacustrine
618 calccrete, southern Portugal. *E3S Web Conf* 98:06012.
619 <https://doi.org/10.1051/e3sconf/20199806012>
- 620 34. Rodrigues AL, Dias MI, Rocha F, et al (2019) Palaeoenvironmental significance
621 and pathways of calccrete development investigated with nuclear and related
622 methods. *J Radioanal Nucl Chem* 321:541–556. [https://doi.org/10.1007/s10967-](https://doi.org/10.1007/s10967-019-06591-w)
623 [019-06591-w](https://doi.org/10.1007/s10967-019-06591-w)
- 624 35. Marques R, Jorge A, Franco D, et al (2010) Clay resources in the Nelas region
625 (Beira Alta), Portugal. A contribution to the characterization of potential raw
626 materials for prehistoric ceramic production. *Clay Miner* 45:353–370.
627 <https://doi.org/10.1180/claymin.2010.045.3.353>
- 628 36. Prudêncio MI, Dias MI, Burbidge CI, et al (2016) PGAA, INAA and luminescence
629 to trace the “history” of “The Panoramic View of Lisbon”: Lisbon before the
630 earthquake of 1755 in painted tiles (Portugal). *J Radioanal Nucl Chem* 307:541–
631 547. <https://doi.org/10.1007/s10967-015-4176-4>
- 632 37. Sanderson DCW, Bishop P, Houston I, Boonsener M (2001) Luminescence
633 characterisation of quartz-rich cover sands from NE Thailand. *Quat Sci Rev*

- 634 20:893–900. [https://doi.org/10.1016/S0277-3791\(00\)00014-7](https://doi.org/10.1016/S0277-3791(00)00014-7)
- 635 38. Burbidge CI, Sanderson DCWW, Housley RA, et al (2007) Survey of Palaeolithic
636 sites by luminescence profiling, a case study from Eastern Europe. *Quat*
637 *Geochronol* 2:296–302. <https://doi.org/10.1016/j.quageo.2006.05.024>
- 638 39. Rodrigues AL, Burbidge CI, Dias MI, et al (2013) Luminescence and mineralogy
639 of profiling samples from negative archaeological features. *Mediterr Archaeol*
640 *Archaeom* 13:37–47
- 641 40. Odriozola CP, Burbidge CI, Dias MI, et al (2014) Dating of Las Mesas Copper
642 Age walled enclosure (La Fuente, Spain). *Trab Prehist* 71:343–352.
643 <https://doi.org/10.3989/tp.2014.12138>
- 644 41. Sanderson DCW, Bishop P, Stark MT, Spencer JQ (2003) Luminescence dating of
645 anthropogenically reset canal sediments from Angkor Borei, Mekong Delta,
646 Cambodia. *Quat Sci Rev* 22:1111–1121. [https://doi.org/10.1016/S0277-](https://doi.org/10.1016/S0277-3791(03)00055-6)
647 [3791\(03\)00055-6](https://doi.org/10.1016/S0277-3791(03)00055-6)
- 648 42. Burbidge CI (2015) A broadly applicable function for describing luminescence
649 dose response. *J Appl Phys* 118:044904. <https://doi.org/10.1063/1.4927214>
- 650 43. Aitken MJ (1999) Archaeological dating using physical phenomena. *Reports Prog*
651 *Phys M J Aitken Rep Prog Phys* 62:1333–1376. [https://doi.org/10.1088/0034-](https://doi.org/10.1088/0034-4885/62/9/202)
652 [4885/62/9/202](https://doi.org/10.1088/0034-4885/62/9/202)
- 653 44. Duller GAT (2003) Distinguishing quartz and feldspar in single grain
654 luminescence measurements. *Radiat Meas* 37:161–165.
655 [https://doi.org/10.1016/S1350-4487\(02\)00170-1](https://doi.org/10.1016/S1350-4487(02)00170-1)
- 656 45. Murray AS, Wintle AG (2003) The single aliquot regenerative dose protocol:
657 Potential for improvements in reliability. *Radiat Meas* 37:377–381.
658 [https://doi.org/10.1016/S1350-4487\(03\)00053-2](https://doi.org/10.1016/S1350-4487(03)00053-2)
- 659 46. Murray AS, Wintle AG (2000) Luminescence dating of quartz using an improved
660 single-aliquot regenerative-dose protocol. *Radiat Meas* 32:57–73.
661 [https://doi.org/10.1016/S1350-4487\(99\)00253-X](https://doi.org/10.1016/S1350-4487(99)00253-X)
- 662 47. Duller GAT (2015) The Analyst software package for luminescence data:
663 overview and recent improvements. *Anc TL* 33:35–42
- 664 48. AMC (2002) Analytical Methods Committee. *RobStat.xla*

- 665 49. Prescott JR, Stephan LG (1982) The contribution of cosmic radiation to the
666 environmental dose for thermoluminescence dating. Latitude, altitude and depth
667 dependences. *Counc Eur PACT J* 6:17–25
- 668 50. Prescott JR, Hutton JT (1988) Cosmic ray and gamma ray dosimetry for TL and
669 ESR. *Nucl Tracks Radiat Meas* 14:223–227. [https://doi.org/10.1016/1359-](https://doi.org/10.1016/1359-0189(88)90069-6)
670 [0189\(88\)90069-6](https://doi.org/10.1016/1359-0189(88)90069-6)
- 671 51. Adamiec G, Aitken M (1988) Dose rate conversion factors. *Anc TL* 16:37–50
- 672 52. Richter D, Zink AJC, Przegietka KR, et al (2003) Source calibrations and blind
673 test results from the new Luminescence Dating Laboratory at the Instituto
674 Tecnológico e Nuclear, Sacavém, Portugal. *Anc TL* 21:43–48
- 675 53. Marques R, Prudêncio MI, Russo D, et al (2021) Evaluation of naturally occurring
676 radionuclides (K, Th and U) in volcanic soils from Fogo Island, Cape Verde. *J*
677 *Radioanal Nucl Chem* 330:347–355. <https://doi.org/10.1007/s10967-021-07959-7>
- 678 54. Zimmerman DW (1971) Thermoluminescent dating using fine grains from pottery.
679 *Archaeometry* 13:29–52. <https://doi.org/10.1111/j.1475-4754.1971.tb00028.x>
- 680 55. Volzone C, Ortiga J (2011) SO₂ gas adsorption by modified kaolin clays:
681 Influence of previous heating and time acid treatments. *J Environ Manage*
682 92:2590–2595. <https://doi.org/10.1016/j.jenvman.2011.05.031>
- 683 56. Dias MI, Rodrigues AL, Kovács I, et al (2020) Chronological assessment of della
684 Robbia sculptures by using PIXE, neutrons and luminescence techniques. *Nucl*
685 *Instruments Methods Phys Res Sect B Beam Interact with Mater Atoms* 477:77–
686 79. <https://doi.org/10.1016/j.nimb.2019.10.008>
- 687 57. Dias MI, Prudêncio MI, Kasztovszky Z, et al (2017) Nuclear techniques applied to
688 provenance and technological studies of Renaissance majolica roundels from
689 Portuguese museums attributed to della Robbia Italian workshop. *J Radioanal Nucl*
690 *Chem* 312:205–219. <https://doi.org/10.1007/s10967-017-5235-9>
- 691 58. Delgado-Raack S (2018) A technological and functional study of the macrolithic
692 artefacts. In: Rafel Fontanals N, Hunt MA, Soriano I, Delgado-Raack S (eds)
693 Prehistoric Copper Mining in the Northeast of the Iberian Peninsula: La Turquesa
694 or Mas de Les Moreres Mine (Cornudella de Montsant, Tarragona, Spain). *Revista*
695 *d'Arqueologia de Ponent*, Número extra 3, Universitat de Lleida, Lleida, pp 47–61

- 696 59. Montero-Ruiz I, Rafel N, Rovira MC, et al (2012) El cobre de Linares (Jaén) como
697 elemento vinculado al comercio fenicio en El Calvari de El Molar (Tarragona).
698 Menga, *Rev Prehist Andalucía* 3:167–184
- 699 60. Rafel N, Soriano I, Armada XL, et al (2019) Lead and copper mining in Priorat
700 county (Tarragona, Spain): From cooperative exchange networks to colonial trade
701 (2600-500 BC). In: Armada XL, Murillo-Barroso M, Charlton M (eds) *Metals,*
702 *minds and mobility: Integrating scientific data with archaeological theory.* Oxbow
703 Books, Oxford, United Kingdom
704